Research Article

Evaluation of Regional Left and Right Ventricular Function in Patients with Ostium-Secundum Atrial Septal Defect Using Speckle Tracking Echocardiography

Toan Pham[a,b], Guillermo Bracamontes-Castelo[c], Neftali Eduardo Antonio-Villa[d], Leonel Avendaño-Pérez[c], Karina del Valle Zamora[e], Candace Keirns[f], Enrique Berrios-Barcenas[e], Nilda Espinola-Zavaleta[g,h*]

[a]Auckland Bioengineering Institute, University of Auckland, Auckland, New Zealand

[b]Department of Physiology, University of Auckland, Auckland, New Zealand

[c]Autonomous University of Baja California, School of Medicine, Mexicali, Baja California, Mexico

[d]MD/PhD Program (PECEM), School of Medicine, Universidad Nacional Autónoma de México, Mexico City, Mexico

[e]Out-patient Clinic, National Institute of Cardiology Ignacio Chavez, Mexico City, Mexico

[f]International Medical Interpreters Association, Boston, MA, USA

[g]Department of Nuclear Cardiology, National Institute of Cardiology Ignacio Chavez, Mexico City, Mexico

[h]Department of Echocardiography, A.B.C. Medical Center I.A.P., Mexico City, Mexico

***Corresponding author:** Nilda Espinola-Zavaleta, Department of Nuclear Cardiology, National Institute of Cardiology Ignacio Chavez, Mexico City, Mexico, E-mail: niesza2001@hotmail.com

Received: 02 July 2020; **Accepted:** 09 July 2020; **Published:** 14 July 2020

Citation: Toan Pham, Guillermo Bracamontes-Castelo, Neftali Eduardo Antonio-Villa, Leonel Avendaño-Pérez, Karina del Valle Zamora, Candace Keirns, Enrique Berrios-Barcenas, Nilda Espinola-Zavaleta. Evaluation of Regional Left and Right Ventricular Function in Patients with Ostium-Secundum Atrial Septal Defect Using Speckle Tracking Echocardiography. Archives of Clinical and Biomedical Research 4 (2020): 274-291.

Abstract

The aim of this study was to provide evidence of abnormalities of right ventricular (RV) and left ventricular (LV) function using speckle tracking echocardiography (STE) in adults with ostium secundum-atrial septal defect (OS-ASD) and pulmonary hypertension (PH).

Sixty-three adult patients with OS-ASD were enrolled. Control group (n=10) with mean pulmonary arterial pressure (MPAP) ≤25 mmHg. Three PH groups were divided based on pulmonary artery systolic pressure (PASP): mild (n=18), moderate (n=24) and severe (n=11). RV free wall strain (RVFWS) and LV global longitudinal strain (LVGLS) were measured.

RVFWS and RV fractional area change were significantly lower in the severe PH group. No difference was found in LVGLS among groups. The moderate PH group had significantly higher right atrial (RA) volume and RV impaired relaxation. RVFWS had a positive correlation with PASP and MPAP.

STE is a valuable non-invasive technique to assess RV and LV systolic function in patients with OS-ASD.

Keywords: Atrial septal defect; Pulmonary hypertension; Strain; Congenital heart disease; Echocardiography; Speckle tracking

Introduction

Atrial septal defect (ASD) is one of the most common congenital heart diseases with a probability of survival into adulthood of up to 97% [1,2]. It is characterized by left-to-right shunting, which often results in right ventricular (RV) volume overload. This can lead to the development of pulmonary hypertension (PH) [3-6] and ultimately RV failure [7,8]. Early detection of RV dysfunction is critical to preventing its deterioration, and RV deformation imaging is a valuable means of providing direct and objective evidence of early ventricular dysfunction in patients with congenital heart disease which is characterized by strain on the RV free wall [9-13]. Speckle tracking echocardiography (STE) has recently been recognized as a powerful tool that can provide noninvasive assessment of right and left ventricular (RV, LV) function with high temporal resolution, independent of the angle and ventricular geometry [14]. STE measures tissue deformation within the myocardium and is expressed as a percentage change. Early diagnosis of PH in a patient with ASD is critical to assess right ventricular function, which can improve the prognosis of these patients. There is a high degree of ventricular interdependency due to the interaction of the interventricular septum during contraction [15]. In the PH disease setting, the RV undergoes hypertrophy and has direct consequences on the left ventricle. Both clinical and experimental observations have demonstrated several anomalies in the LV myocardium, including atrophic remodeling and reduced peak LV systolic pressure [16,17]. However, no information is available about the direct measurement of interventricular function in adults with OS-ASD. The present study aimed to investigate abnormalities of RV and LV function using speckle tracking echocardiography in adults with OS-ASD and varying degree of PH.

Materials and Methods

Study population

Eighty-four adult patients with OS-ASD were assessed for a cross-sectional and analytical echocardiographic study from March 2015 to October 2017. Exclusion criteria included mitral, aortic, tricuspid and pulmonic valve lesions

(n=3), additional congenital heart diseases (n=7), coronary artery disease (n=4), heart failure (n=2) and poor acoustic window (n=5). We approached and consecutively evaluated the remaining 63 patients in the Out-patient Clinic of the National Institute of Cardiology Ignacio Chavez. The protocol of this study included twelve-lead resting electrocardiograms and conventional and speckle tracking echocardiograms. When the echocardiograms were performed, the patients were not receiving medical treatment.

All patients had complete clinical histories and signed consent forms. The study design was approved by the Ethics Committee of the National Institute of Cardiology Ignacio Chavez and the protocol number is 15-921.

Echocardiographic evaluation

Conventional transthoracic echocardiographic studies were performed using Vivid 9X-clear equipment (GE Vingmed Ultrasound, Horten, Norway). The left ventricular ejection fraction (LVEF) was calculated using four and two-chamber apical views by the modified Simpson method. LVEF was considered normal, when it was ≥52% for men and ≥ 54% for women. The E and A wave velocities were measured with pulsed Doppler in the apical four-chamber plane, placing the sample volume at the tips of the mitral leaflets. Left atrial (LA) volume was calculated with the area-length method in the apical four-chamber view and two-chamber view at end systole and it was indexed by body surface area. The upper normal limit for LA volume index is 34 mL/m^2.

Diastolic function was evaluated using pulsed Doppler in the apical four-chamber plane with the sample volume placed at the tips of the mitral leaflets. E- and A-wave velocities (rapid filling and atrial contribution, respectively) and E/A ratio were assessed.

Right ventricular end-diastolic diameter was measured in the apical four-chamber view, above the tricuspid valve; the normal value was ≤43 mm. The RV wall thickness was measured by 2D echocardiography in the subcostal four chamber view. A value ≥ 0.5 cm was considered abnormal. The right ventricular fractional area change (RVFAC) was calculated in the apical four-chamber plane using the following formula: (end-diastolic area - end-systolic area/end-diastolic area) ×100. The normal value was ≥35%. The tricuspid annular plane systolic excursion (TAPSE) was measured using M-mode in the apical four- chamber plane, and a value of ≥16 mm was considered normal. The tricuspid S-wave velocity was measured by tissue Doppler imaging, placing the sample volume at the basal portion of the RV free wall in the apical four-chamber plane and the normal value was ≥9.5 cm/s. Tei index was calculated by tissue Doppler velocity of the lateral tricuspid annulus, in the apical four-chamber view, and a value <0.54 was considered normal. Diastolic function was assessed using pulsed Doppler in the apical four-chamber plane with the sample volume placed at the tips of the tricuspid leaflets. E- and A-wave velocities (rapid filling and atrial contribution, respectively) and E/A ratio were obtained. A ratio of tricuspid E/ e´ of the lateral tricuspid annulus was measured for assessment of right ventricular diastolic function, and the normal ratio was ≥6.2.

Right atrial (RA) volume was obtained using a single-plane method of disks, in the apical four-chamber view at end systole and it was indexed by body surface area. The normal RA volume index is 25 ± 7mL/m^2.

All the echocardiographic measurements were made according to the guidelines of the American Society of Echocardiography and the European Association of Cardiovascular Imaging [18-20].

Measurements of the interatrial septal defect were made in the 4-chamber subcostal plane along its long axis and in the modified apical four-chamber view by sliding the transducer medially from the apical four-chamber view toward the sternal border. The shunt and its hemodynamic impact, across the ostium OS-ASD was assessed through a combination of 2D-bidimensional, color flow Doppler and pulsed wave Doppler. The shunt flow was estimated by pulsed Doppler of the pulmonary (Qp) to systemic (Qs) blood flow ratio. For quantification of the Qp/Qs ratio, the systolic velocity time integrals (VTIs) of the RV and LV outflow, and the maximal systolic diameters of the pulmonary and LV outflow tracts were measured. The estimation of the RV and LV outflow tract area (πr^2) multiplied by the corresponding VTI provided the stroke volume for the right and left ventricles, respectively. The Qp/Qs ratio was the ratio of the pulmonary to systemic stroke volumes (RV stroke volume/LV stroke volume) [21,22].

Pulmonary arterial pressure assessment

The pulmonary artery systolic pressure (PASP) was calculated by tricuspid regurgitation velocity with continuous-wave Doppler in the apical four-chamber view, using the simplified Bernoulli equation: PASP = 4 × (maximal TR velocity)^2 + right atrial pressure (RAP). RAP was estimated in the subcostal view according to the inferior vena cava (IVC) size and collapsibility following a normal sniff: An IVC diameter < 2.1 cm that collapsed >50% with a sniff suggested normal RA pressure of 3 mm Hg (range, 0–5 mm Hg), whereas an IVC diameter > 2.1 cm that collapsed < 50% with a sniff suggested a high RA pressure of 15 mm Hg (range, 10–20 mm Hg). In scenarios in which IVC diameter and collapse did not fit this paradigm, an intermediate value of 8 mm Hg (range, 5–10 mm Hg) might be used, or, preferably, other indices of RA pressure could be integrated to downgrade or upgrade to the normal or high values of RA pressure [18-20].

The MPAP was determined by echocardiography, using the following formula= 0.60 x PASP + 2.1 mmHg [23]. According to 2015 ESC/ERS guidelines for the diagnosis of pulmonary hypertension (PH) [24], patients with mean pulmonary arterial pressure (MPAP) greater than 25 mm Hg were considered to have PH. There were 10 patients with MPAP lower than 25 mm Hg, and they made up the control group. Using the systolic pulmonary arterial pressure (PASP), patients with PH (n = 53) were further divided into: mild (36-49 mm Hg), moderate (50-70 mm Hg), and severe (>70 mm Hg).

Speckle tracking measurements

The patients were evaluated in the left lateral decubitus, using Vivid 9 X-clear (GE) equipment with software for ventricular mechanics. A region of interest was traced with a point-and-click approach on the endocardium of the RV free wall at the end of diastole in an apical four-chamber view. A larger region of interest was subsequently generated and manually adjusted near the RV epicardium. The program automatically divided the RV free wall into three segments and performed analysis of the deformation frame by frame with a frequency between 50 and 80 frames per sec in deep expiration (Figure 1). This process allowed an automated confirmation of the contour and generated deformation values. The three segments were averaged, and the value was considered to be the RV free wall strain (RVFWS), in which the normal value of RVFWS was given as -29.0 ± 4.5% based on the 2015 ASE/EACVI guidelines [12-14,18-20]. Left ventricular global longitudinal strain (LVGLS) was defined as the average of peak systolic strain values of the 17-segment model and it was assessed in the apical four chamber, two chamber and three chamber views, a LVGLS value <-20% was considered abnormal. The LV circumferential and radial deformation was performed using the short axes at the level of the mitral valve, papillary muscles and apex, where these normal values were more than – 23.3% and +40%, respectively [18,25].

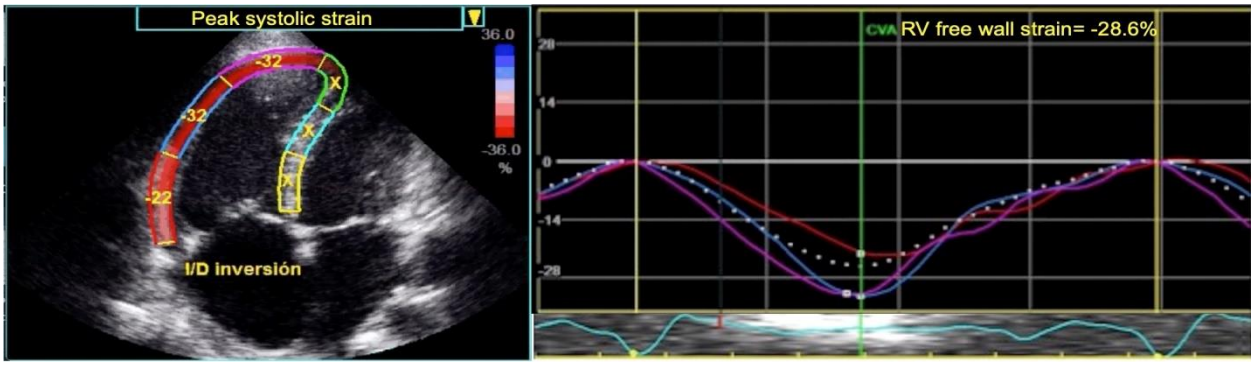

Figure 1: Measurement of RV peak systolic strain by 2D STE, averaged over the three segments of the RV free wall in RV-focused apical four chamber view, (-28.6%).

Statistical analysis

Continuous data variables were expressed as mean (±standard deviation) or median (interquartile range) according if the data followed normal distribution using the Kolmogorov-Smirnov test if they did not. To assess differences between groups of PH, we performed an ANOVA or a Kruskal-Wallis test wherever appropriate. Further comparisons among groups were performed using the Tukey or Dunn's post hoc test wherever appropriate. To assess the correlation between RVFWS and hemodynamic parameters we used the Pearson's and coefficient analysis. A partial correlation analysis was also performed to adjust for covariates. Aditionally, a non-linear regression analysis was performed to evaluate the best fit to our model between both variables. Both methods were adjusted for age, body superficial area, RV fractional area change and right performance index, which are known covariates that modifies RV function. To predict the optimal cut-off values to predict RV dysfunction based on

PASP we assessed it by evaluating the area under the curve (AUC) of receiver operating characteristic (ROC) curves. The optimal cut-off value was defined as closest to 1 in the top left corner, using the Youden method. The ROC curve of RVFWS was compared against those of the conventional transthoracic echocardiographic parameters (tricuspid annular plane systolic excursion, S wave velocity, RV performance index, and RV fractional area change). Finally, the intra and interobserver variability was assessed in 12 patients. We extracted the intraclass correlation coefficients using the average measures of the PASP, MPAP and RV and LV strains between previously obtained measurements and the actual measurements. A second independent echocardiographer who was not involved in the first measurements performed the echocardiographic evaluation of the previously mentioned parameters. All statistical analyses were performed with the Social Package for Social Sciences (SPSS, version 23) and the graphs were done using GraphPad Prism (Version 8.0). A p value ≤ 0.05 was considered as statistically significant.

Results

Patient characteristics

Demographic and clinical characteristics of the study population are presented in Table 1. Briefly, we included 63 patients with previous diagnoses of OS-ASD, 49 (77.7%) were female and 53 with PH (84%). Our control group consisted of 10 (15.8%) patients without PH. Further classification of PH included: 18 (28.5%) with mild, 24 (38%) with moderate and 11 (17.5%) patients with severe PH. Patients with moderate PH were significantly older than the control and mild PH groups.

Table 1: Demographic findings of adult ASD patients with PH

Parameters	**Control (n = 10)**	**Mild PH (n = 18)**	**Moderate PH (n = 24)**	**Severe PH (n = 11)**
Age (years)	33.2 ± 9.1	33.7 ± 13.0	48.8 ± 13.6*,#	47.5 ± 16.0
Women (n, %)	6 (60.0%)	13 (72.2%)	20 (83.3%)	10 (90.9%)
Weight (kg)	69.3 ± 12.3	65.3 ± 14.0	64.6 ± 13.2	67.3 ± 13.73
Height (m)	1.61 ± 0.10	1.62 ± 0.10	1.54 ± 0.08#	1.54 ± 0.06
BMI (kg/m^2)	26.7 ± 3.8	24.8 ± 4.1	27.1 ± 4.6	28.4 ± 6.5
BSA (cm^2/m^2)	1.74 ± 0.19	1.68 ± 0.20	1.64 ± 0.20	1.67 ± 0.15
NYHA Functional class				
1 (n, %)	5 (50%)	14 (77.8%)	15 (62.5%)	1 (9.1%)
2 (n, %)	5 (50%)	4 (22.2%)	8 (33.3%)	10 (90.9%)
3 (n, %)	0	0	1 (4.2%)	0
PSAP (mm Hg)	34.1 ± 2.0	43.2 ± 3.5*,#,&	57.7 ± 5.1#,&	92.6 ± 17.5&
PMAP (mm Hg)	22.7 ± 1.2	28.5 ± 2.4*,#,&	37.2 ± 3.1#,&	58.9 ± 11.0&

Abbreviations: ASD: atrial septal defect, BMI: body mass index, BSA: body surface area, PH: pulmonary hypertension, MPAP: mean pulmonary arterial pressure, PASP: pulmonary artery systolic pressure. Values are expressed as mean ± SD. The * symbol denotes p<0.05 when severe PH was compared to controls, the '#' symbol when p<0.05 comparing severe PH to mild PH, and the '&' symbol when p<0.05 comparing severe PH to moderate PH.

Echocardiographic evaluation

Echocardiographic evaluation among our groups of study are presented in Table 2. RV free wall thickness, tricuspid E/e' and RV RVFAC were all significantly greater in the severe PH group compared to control, mild and moderate groups. The moderate PH group showed significantly higher values of right atrial volume and E/A tricuspid ratio compared to the control group. There were no differences in TAPSE, S wave velocity, RV performance index and LVEF among groups.

Table 2: Echocardiographic characteristics

Parameters	Control (n = 10)	Mild PH (n = 18)	Moderate PH (n = 24)	Severe PH (n = 11)
LA volume (ml/m^2)	29.5 ± 5.9	31.6 ± 10.4	34.8 ± 10.4	34.1± 12.2
RA volume (ml/m^2)	40.1 ± 10.5	50.8 ± 14.6	69.3 ± 32.9*	66.1 ± 24.2
RV thickness (mm)	5.5 ± 0.7	6.4 ± 1.3	6.9 ± 1.3	8.6 ± 2.6*,#,&
RV basal diameter (mm)	49.5 ± 6.5	50.8 ± 6.7	51.8 ± 7.0	51.4 ± 5.7
RV medial diameter (mm)	44.7 ± 8.0	44.1 ± 7.5	47.0 ± 6.1	46.2 ± 5.8
RV longitudinal diameter (mm)	77.5 ± 9.0	80.5 ± 8.8	77.7 ± 9.6	79.0 ± 7.7
RVFAC (%)	42.3 ± 6.9	44.6 ± 9.2	37.9 ± 4.7#	31.5 ± 7.5*,#
TAPSE (mm)	26.8 ± 6.3	25.3 ± 4.8	24.2 ± 4.1	22.1 ± 5.9
S wave velocity (cm s-1)	14.8 ± 3.5	14.3 ± 2.7	13.7 ± 3.2	12.7 ± 1.8
RV performance index	1.8 ± 0.5	1.5 ± 0.6	1.4 ± 0.7	1.3 ± 0.7
E tricuspid wave	0.67 ± 0.22	0.75 ± 0.26	0.57 ± 0.21	0.55 ± 0.22
A tricuspid wave	0.55 ± 0.28	0.62 ± 0.23	0.68 ± 0.28	0.67 ± 0.27
E/A tricuspid ratio	1.3 ± 0.3	1.3 ± 0.4	0.9 ± 0.3#	1.0 ± 0.5
Tricuspid E/e'	8.0 ± 2.9	7.9 ± 1.8	9.8 ± 3.0	12.3 ± 5.4*,#
ASD diameter (mm)	27.3 ± 6.2	27.6 ± 6.2	33.1 ± 8.8	30.4 ± 7.5
Shunt	2.5 ± 0.5	2.8 ± 0.8	3.2 ± 1.0	2.8 ± 1.0
LV end-diastolic volume (ml)	110.5 ± 19.2	114.5 ± 14.4	122.4 ± 12.1	124.2 ± 15.3

LV end-systolic volume (ml)	48.2 ± 2.2	49.1 ± 2.3	50.1 ± 5.2	52.1 ± 3.2
LV ejection fraction (%)	62.4 ± 7.2	63.51 ± 6.3	65.21 ± 7.7	65.81 ± 5.9
E/A mitral ratio	1.3 ± 0.3	1.3 ± 0.4	1.1 ± 0.6	0.9 ± 0.4

Abbreviations: RVFAC: right ventricular fractional area change, ASD: atrial septal defect, LA: left atrium, LV: left ventricle, PH: Pulmonary hypertension, RA: right atrium, RV: right ventricle, TAPSE: tricuspid annular plane systolic excursion. Values are expressed as mean ± SD. The * symbol denotes $p<0.05$ when severe PH was compared to controls, the '#' symbol $p<0.05$ when comparing severe PH to mild PH, and the '&' symbol $p<0.05$ when comparing severe PH to moderate PH

Ventricular and atrial deformation parameters

We found that RVFWS and septal longitudinal strain were significantly decreased in the severe PH group compared to control and mild PH groups (Table 3, Figure 2A). However, no differences were detected in LVGLS (Figure 2B), LV global circumferential strain (LVGCS, Figure 2C) and LV global radial strain (LVGRS), among control and PH groups. In our correlation analysis, we found that RVFWS was positively correlated with PASP (r = 0.402; 95% CI: 0.316-0.490) (Figure 2A) and MPAP (r = 0.415; 95% CI: 0.328-0.502*)* and found that RVFWS explained the 20% and 20.4% of the variability of both measurements, respectively. (Figure 3, Supplementary Table 1).

Table 3: Parameters of RV and LV mechanical deformations

Parameters	**Control (n = 10)**	**Mild PH (n = 18)**	**Moderate PH (n = 24)**	**Severe PH (n = 11)**
RV FWS (%)	-26.3 ± 5.2	-26.3 ± 5.2	-26.7 ± 6.0	-18.9 ± 8.2 $^{*,\#,\&}$
Septal LS (%)	-26.2 ± 4.3	-23.7 ± 6.5	-24.4 ± 4.0	-17.2 ± 7.6 $^{*,\#,\&}$
LV GLS (%)	-22.3 ± 3.2	-21.7 ± 3.1	-23.0 ± 3.5	-22.8 ± 4.0
LV GCS (%)	-19.5 ± 4.1	-16.2 ± 9.3	-18.0 ± 4.6	-18.8 ± 3.3
LV GRS (%)	40.6 ± 10.7	41.9 ± 6.8	36.0 ± 10.5	34.3 ± 13.1

Abbreviations: RL FWS: right ventricular free wall strain, Septal LS: septal longitudinal strain, LVGLS: left ventricular global longitudinal strain, LVGCS: left ventricular global circumferential strain, LV GRS: left ventricular global radial strain. Values are expressed as mean ± SD. The * symbol denotes $p<0.05$ when severe PH was compared to controls, the '#' symbol $p<0.05$ when comparing severe PH to mild PH, and the '&' symbol $p<0.05$ when comparing severe PH to moderate PH.

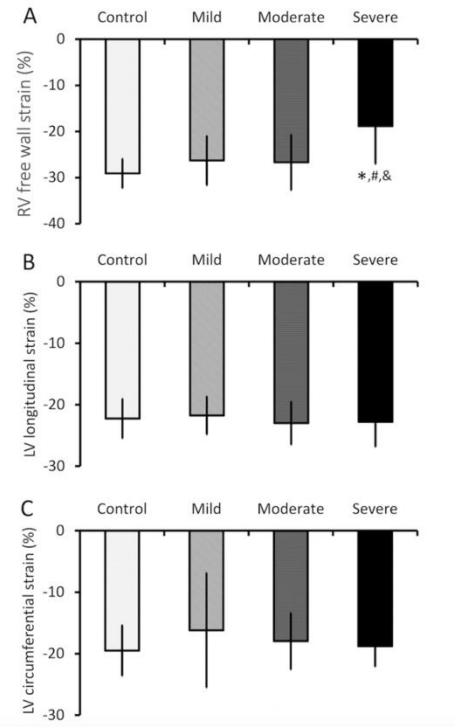

Figure 2: Comparison of mechanical deformation among PH groups. (A) RV free wall strain, (B) LV global longitudinal strain, and (C) LV global circumferential strain from the control and three PH groups. Values are means ± SD. The * symbol denotes $p<0.05$ when severe PH was compared to controls, the '#' symbol when $p<0.05$ comparing severe PH to mild PH, and the '&' symbol when $p<0.05$ comparing severe PH to moderate PH. LV: Left ventricular, PH: Pulmonary hypertension, RV: Right ventricular, SD: Standard deviation.

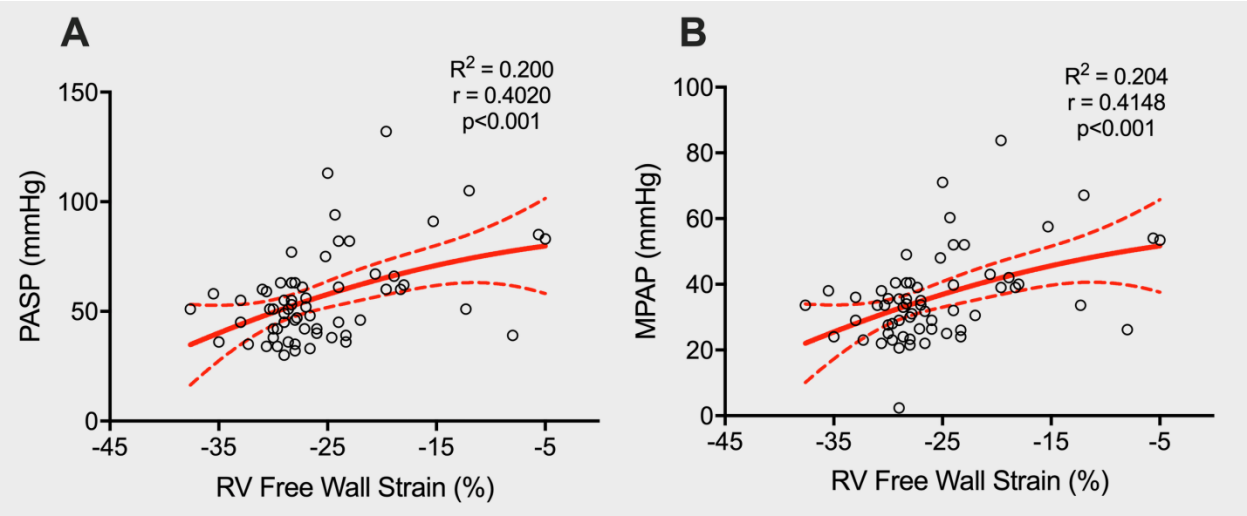

Figure 3: Correlations of RVFWS with pulmonary artery systolic pressure (A; PASP), and mean pulmonary arterial pressure (B; MPAP). Red line represents the predicted values according to the quadratic fit between each variable.

Supplementary Table 1: Unadjusted and adjusted correlation and regression analyses for RV longitudinal strain with PASP and MPAP. Covariates for the adjusted models: age, body superficial area, right ventricular fractional area change, and right performance index.

Parameter	**Un-adjusted**		**Adjusted**	
RV Free Wall Strain	PASP	MPAP	PASP	MPAP
Correlation coefficient	0.402 (0.218-0.622)	0.415 (0.193-0.615)	0.350 (0.098-0.559)	0.338 (0.084-0.550)
Non-linear regression analysis				
B-coefficient	1.377	0.906	0.976	0.630
R^2	0.200	0.204	0.381	0.348

Abbreviations: PASP= Pulmonary artery systolic pressure; MPAP= Mean pulmonary arterial pressure.

Finally, exploring the capacity of RVFWS and conventional transthoracic echocardiographic parameters (RV FAC, TAPSE, RV performance, S wave velocity) to predict RV dysfunction based on the PSAP, we found that RVFWS (AUC: 0.801; 95% CI: 0.684-0.918, p<0.0001) and RV fractional area change (AUC: 0.800; 95% CI: 0.691-0.906, p<0.0001) were useful predictors of RV dysfunction in PASP≥ 60 mmHg (value selected based on the accepted cut-off point in the literature). The first with a cut-off value less than -25.6% presents a better specificity (83%) and the second with a cut-off value of less than 38% presents better sensitivity (81%), (Table 4, Figure 4).

Table 4: AUCs indicating the ability of RV free wall longitudinal strain and conventional transthoracic echocardiographic parameters (RV fractional area change, TAPSE; RV performance index, S wave velocity) to predict RV dysfunction based on PASP ≥60 mmHg.

Parameters	**AUC**	**95% CI**	***P value***
RV fractional area change	0.800	*0.691-0.906*	*P* < 0.0001
TAPSE	0.595	*0.447-0.743*	*P* = 0.217
S wave velocity	0.563	*0.418-0.743*	*P* = 0.418
Tei index RV	0.535	*0.384-0.685*	*P* = 0.654
RV FWS	0.801	*0.684-0.918*	*P* < 0.0001

Abbreviations: AUC: Area under the curve, PASP: Pulmonary arterial systolic pressure, RV: Right ventricular, TAPSE: tricuspid annular plane systolic excursion, RV FWS: right ventricular free wall strain. *P* < 0.05 denotes significant difference.

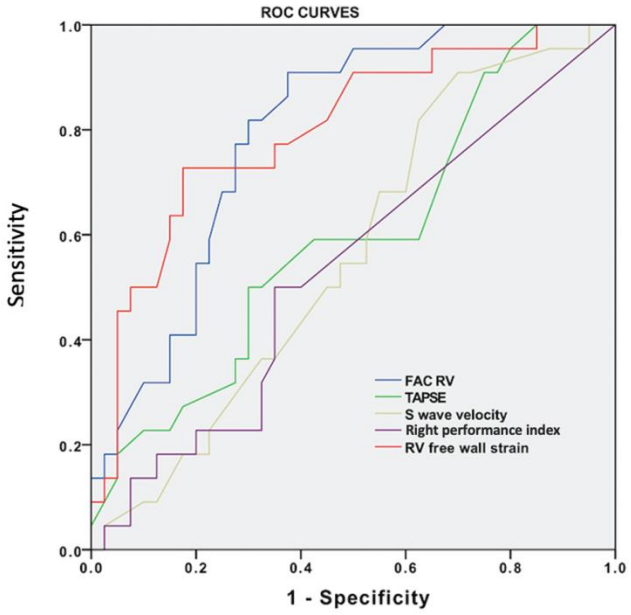

Figure 4: ROC curves exhibiting abilities of RVFWS, RV performance index, S wave velocity, TAPSE and

RVFAC to predict RV dysfunction in patients with OS-ASD with PH. The cut-off point for RVFAC was 38% with sensitivity = 81.8% and specificity = 75% and for RVFWS of -25.6 % with sensitivity = 72.7% and specificity = 82.5%.

OS-ASD: Ostium secundum-Atrial septal defect, PH: Pulmonary hypertension, ROC: Receiver operating characteristic, RV: Right ventricular, TAPSE: Tricuspid annular plane systolic excursion.

We obtained a 0.944 (95% CI 0.677-0.983, $p<0.001$) interclass coefficient, which is a strong indicator that the measurements performed during our study were consistent, independent of the observer.

Discussion

In patients with ASD the elevated levels of PASP are flow dependent, caused by increased flow on the right side owing to the left-to-right shunt. Severe PH in patients with significant atrial shunts usually develops more slowly as a response to the increased pulmonary blood flow with remodeling of the pulmonary arteries [26,27].

In this study, we investigated abnormalities of RV and LV function using speckle tracking echocardiography in adults with ostium secundum ASD and varying degrees of PH. We did not find any statistically significant differences among any RV diameters; furthermore, only those with severe PH had increased RV thickness compared to our control group.

We found that the RV free wall strain and RV fractional area change were decreased in the severe PH group compared to the control group, but no effect on LVGLS was detected among the control and the three PH groups. We also observed no difference in LV ejection fraction among three PH groups compared to the control group, but type I diastolic dysfunction (impaired relaxation) was observed mainly in the group with severe PH. These findings were consistent with those of previous studies that suggested that global two-dimensional strain could be a better parameter for predicting clinical events in acute heart failure than LV ejection fraction [28]. It is important to mention, that there are no universal normal values for strain. The strain values vary substantially from vendor to vendor, and for this reason the EACVI and ASE initiated the Strain Standardization Task Force to develop an academic-industrial consortium that could reach a consensus on a list of standard definitions and nomenclature for the clinical parameters evaluated with 2D speckle tracking technology and to create a common standard [29].

The results indicate that chronic RV pressure overload in PH patients directly affects the systolic performance of the right ventricle but not the left ventricle. Moreover, RVFWS had a positive correlation in a non-linear (quadratic) fit with PASP and MPAP. Furthermore, these were not attributable to larger volumes or larger ventricular size as we did not find differences in our groups; thus, they correlated with the pathophysiological mechanisms that explained that RV dysfunction leads to a decreased PASP and MPAP. This suggests that RVFWS could potentially be used to evaluate the RV function in patients with OS-ASD and PH. RVFWS was a better index of RV function than TAPSE, MPI, S wave velocity or RVFAC.

Additionally, RV impaired relaxation and a significantly higher tricuspid E/e´ ratio were found in patients with OS-ASD and moderate to severe HP compared to controls and those with mild PH, indicating an increase in RV filling pressure. Cossio-Aranda et al. (2016) found that tricuspid E/e' ratio>6.2 is a predictor of right ventricular diastolic dysfunction in patients with OS-ASD [30]. Utsunomiya *et al.* [31] also demonstrated that tricuspid E/e´ is a powerful predictor of cardiac events in patients with chronic PH, suggesting the prognostic importance of RV diastolic dysfunction.

Furthermore, we used speckle tracking echocardiography to assess regional RV function. It is known that during systolic contraction, RV longitudinal shortening provides the predominant contribution to ejection of blood, rather than circumferential shortening [32]. Thus, the measurement of RVFWS has been proposed as a useful means of examining RV hemodynamic changes in healthy individuals and in patients living with PH [9,10]. In our results, we found that RVFWS was significantly lower in the severe PH group. This is consistent with previous findings of lower RV lateral wall global longitudinal strain in ASD patients compared to controls [11]. Interestingly, these investigators showed that patients who already had undergone surgery in childhood demonstrated a decrease in peak systolic RVFWS [11]. We hypothesize that the decreased RVFWS is a compensatory consequence of chronic volume overload prior to surgical closure. This supposition is supported by the fact that severe PH patients with no medical history of ASD also exhibited the decrease of RVFWS [9,14,33,34]. However, a previous study using a similar imaging technique has reported significantly higher RVFWS from ASD patients compared to the control group and the RVFWS was reduced in the same patients after ASD closure [35]. We are aware of such discrepancies; the control group in our study had ASD, and that could explain the higher RVFWS values of our control group compared to their group.

We found that the RVFAC was significantly lower in the severe PH group. This was in agreement with a prior study of severe PH patients with OS-ASD using two-dimensional echocardiography [36]. The decrease in RVFAC could be directly comparable to our previous finding using a rodent PH model that demonstrated a decrease in the extent of shortening in isolated RV muscles from the PH group compared to the control group. The mechanism underlying diminished shortening could be decreased velocity of shortening [14,37] as a result of a shift in the myosin heavy chain from fast to slow [38-40] and increased fibrosis in the RV myocardium in the PH model [41].

A noteworthy contribution of this study was the evaluation of regional LV function in OS-ASD patients with varying degrees of PH. Our results revealed no differences in global longitudinal, circumferential and radial strain in the LV among three PH groups compared to the control group. This finding aligns with a previous study of ASD patients that reported no difference in LV global and segmental longitudinal strain compared to controls [11]. We also note that comparable results of no difference in circumferential fiber shortening are consistent with those seen in a previous study on PH patients with no ASD [42].

RVFWS had a positive correlation with PASP. This is in agreement with a previous study [9] and supports the value of RVFWS for the assessment of RV systolic function using speckle tracking echocardiography.

Limitation

Our study included a small number of patients in a prospective single center study; larger populations in future studies will be necessary to determine the utility of RVFWS for evaluating RV systolic function. A second limitation is the inclusion of patients of different genders in the same group. There was a greater proportion of female patients in this study. Gender differences exist in the prevalence of PH [43-46] with a striking female-to-male ratio of nearly 4-to-1. A gender comparison study will be crucial for future scientific consideration. Third, right heart catheterization was not included in this study. Inasmuch as catheterization is the gold standard for differentiating precapillary pulmonary hypertension from post-capillary PH.

Fourth, in patients with very severe TR, the Doppler envelope may be cut off because of an early equalization of RV and RA pressures, and the simplified Bernoulli equation may underestimate the RV-RA gradient.

Conclusion

Patients with ostium secundum-ASD and PH develop RV systolic dysfunction and biventricular diastolic dysfunction. Speckle tracking echocardiography is a valuable non-invasive technique to assess RV and LV systolic function in these patients.

Abnormal RVFWS can be a useful predictor of the severity of PH in adult patients with OS-ASD.

Acknowledgments

The authors would like to thank the entire staff of the Nuclear Cardiology Department at Instituto Nacional de Cardiologia Ignacio Chavez, particularly the nurses and technicians. Neftali Eduardo Antonio-Villa is enrolled in the PECEM program of the Faculty of Medicine at UNAM and its supported by CONACYT.

Conflict of Interests

The authors declare that they have no conflict of interests.

References

1. Moons P, Bovijn L, Budts W, Belmans A, Gewillig M. Temporal trends in survival to adulthood among patients born with congenital heart disease from 1970 to 1992 in Belgium. Circulation 122 (2010): 2264-72.

2. Rosas M, Attie F, Sandoval J, Castellano C, Buendia A, Zabal C, Granados N. Atrial septal defect in adults > or =40 years old: negative impact of low arterial oxygen saturation. Int J Cardiol 93 (2004): 145-55.
3. Vogel M, Berger F, Kramer A, Alexi-Meshkishvili V, Lange PE. Incidence of secondary pulmonary hypertension in adults with atrial septal or sinus venosus defects. Heart (British Cardiac Society) 82 (1999): 30-3.
4. Post MC. Association between pulmonary hypertension and an atrial septal defect. Netherlands heart journal : monthly journal of the Netherlands Society of Cardiology and the Netherlands Heart Foundation 21 (2013): 331-2.
5. Torres AJ. Hemodynamic assessment of atrial septal defects. J Thorac Dis 10 (2018): S2882-S2889.
6. Zwijnenburg RD, Baggen VJM, Witsenburg M, Boersma E, Roos-Hesselink JW, van den Bosch AE. Risk Factors for Pulmonary Hypertension in Adults After Atrial Septal Defect Closure. Am J Cardiol 123 (2019): 1336-1342.
7. Vonk-Noordegraaf A, Haddad F, Chin KM, Forfia PR, Kawut SM, Lumens J, Naeije R, Newman J, Oudiz RJ, Provencher S, Torbicki A, Voelkel NF, Hassoun PM. Right heart adaptation to pulmonary arterial hypertension: physiology and pathobiology. J Am Coll Cardiol 62 (2013): D22-33.
8. Vonk-Noordegraaf A, Marcus JT, Gan CT, Boonstra A, Postmus PE. Interventricular mechanical asynchrony due to right ventricular pressure overload in pulmonary hypertension plays an important role in impaired left ventricular filling. Chest 128 (2005): 628S-630S.
9. Li Y, Xie M, Wang X, Lu Q, Fu M. Right ventricular regional and global systolic function is diminished in patients with pulmonary arterial hypertension: a 2-dimensional ultrasound speckle tracking echocardiography study. Int J Cardiovasc Imaging 29 (2013): 545-51.
10. D´Andrea A, Caso P, Bossone E, Scarafile R, Riegler L, et al. Right ventricular myocardial involvement in either physiological or pathological left ventricular hypertrophy: an ultrasound speckle-tracking two-dimensional strain analysis. Eur J Echocardiogr 11 (2010): 492-500.
11. Menting ME, van den Bosch AE, McGhie JS, Cuypers JA, Witsenburg M, Geleijnse ML, Helbing WA, Roos-Hesselink JW. Ventricular myocardial deformation in adults after early surgical repair of atrial septal defect. Eur Heart J Cardiovasc Imaging 16 (2015): 549-57.
12. Gecmen C, Candan O, Kahyaoglu M, Kalayci A, Cakmak EO, Karaduman A, Izgi IA, Kirma C. Echocardiographic assessment of right ventricle free wall strain for prediction of right coronary artery proximal lesion in patients with inferior myocardial infarction. Int J Cardiovasc Imaging 34 (2018): 1109-16.
13. Friedberg MK, Mertens L. Deformation imaging in selected congenital heart disease: is it evolving to clinical use? Journal of the American Society of Echocardiography : official publication of the American Society of Echocardiography 25 (2012): 919-31.

14. Pirat B, McCulloch ML, Zoghbi WA. Evaluation of global and regional right ventricular systolic function in patients with pulmonary hypertension using a novel speckle tracking method. Am J Cardiol 98 (2006): 699-704.
15. Naeije R, Badagliacca R. The overloaded right heart and ventricular interdependence. Cardiovasc Res 113 (2007): 1474-1485.
16. Gan CT, Lankhaar JW, Marcus JT, Westerhof N, Marques KM, Bronzwaer JG, Boonstra A, Postmus PE, Vonk-Noordegraaf A. Impaired left ventricular filling due to right-to-left ventricular interaction in patients with pulmonary arterial hypertension. Am J Physiol Heart Circ Physiol 290 (2006): H1528-33.
17. Correia-Pinto J, Henriques-Coelho T, Roncon-Albuquerque R, Lourenco A, Melo-Rocha G, Vasquez-Novoa, Gillebert T, Leite-Moreira A. Time course and mechanisms of left ventricular systolic and diastolic dysfunction in monocrotaline-induced pulmonary hypertension. Basic Res Cardiol 104 (2009): 535-45.
18. Lang RM, Bierig M, Devereux RB, et al. Recommendations for chamber quantification: a report from the American Society of Echocardiography's Guidelines and Standards Committee and the Chamber Quantification Writing Group, developed in conjunction with the European Association of Echocardiography, a branch of the European Society of Cardiology. J Am Soc Echocardiogr, 2005. 18(12): p. 1440-63.
19. Mor-Avi V, Lang RM, Badano LP, Belohlavek M, Cardim NM, et al. Current and Evolving Echocardiographic Techniques for the Quantitative Evaluation of Cardiac Mechanics: ASE/EAE Consensus Statement on Methodology and Indications Endorsed by the Japanese Society of Echocardiography. Eur J Echocardiogr 12 (2011): 167-205.
20. Rudski LG, Lai WW, Afilalo J, Hua L, Handschumacher MD, Chandrasekaran K, Solomon SD, Louie EK, Schiller NB. Guidelines for the echocardiographic assessment of the right heart in adults: a report from the American Society of Echocardiography endorsed by the European Association of Echocardiography, a registered branch of the European Society of Cardiology, and the Canadian Society of Echocardiography. J Am Soc Echocardiogr 23 (2010): 685-713.
21. Kitabatake A, Inoue M, Asao M, Ito H, Masuyama T, Tanouchi J, Morita T, Hori M, Yoshima H, Ohnishi K. Noninvasive evaluation of the ratio of pulmonary to systemic flow in atrial septal defect by duplex Doppler echocardiography. Circulation 69 (1984): 73-9.
22. Silvestry FE, Cohen MS, Armsby LB, , Burkule NJ, Fleishman CE, Hijazi ZM, Lang RM, Rome JJ, Wang Y. Guidelines for the echocardiographic assessment of atrial septal defect and patent foramen ovale: From the American Society of Echocardiography and Society for Cardiac Angiography and Interventions. J Am Soc Echocardiogr 28 (2015): 910-958.
23. Hellenkamp K, Unsold B, Mushemi-Blake S, Shah AM, Friede T, Hasenfuß G, Seidler T. Echocardiographic Estimation of Mean Pulmonary Artery Pressure: A Comparison of Different Approaches to Assign the Likelihood of Pulmonary Hypertension. J Am Soc Echocardiogr 31 (2018): 89-98.

24. Galie N, Humbert M, Vachiery JL, Gibbs S, Lang I, et al. 2015 ESC/ERS Guidelines for the diagnosis and treatment of pulmonary hypertension: The Joint Task Force for the Diagnosis and Treatment of Pulmonary Hypertension of the European Society of Cardiology (ESC) and the European Respiratory Society (ERS): Endorsed by: Association for European Paediatric and Congenital Cardiology (AEPC), International Society for Heart and Lung Transplantation (ISHLT). Eur Respir J 46 (2015): 903-75.
25. Gabriels C, De Meester P, Pasquet A, De Backer J, Paelinck BP, Morissens M, Van De Bruaene A, Delcroix M, Budts W. A different view on predictors of pulmonary hypertension in secundum atrial septal defect. Int J Cardiol 176 (2014): 833-40.
26. Opotowsky AR. Clinical evaluation and management of pulmonary hypertensionhypertension in the adult with congenital heart disease. Circulation 131 (2015): 200-210.
27. Webb G, Gatzoulis MA. Atrial septal defects in the adult. Recent progress and overview. Circulation 114 (2006): 1645-1653.
28. Cho GY, Marwick TH, Kim HS, Kim MK, Hong KS, Oh DJ. Global 2-dimensional strain as a new prognosticator in patients with heart failure. J Am Coll Cardiol 54 (2009): 618-24.
29. Voigt JU, Pedrizzetti G, Lysyansky P, Marwick TH, Houle H, et al. Definitions for a common standard for 2D speckle tracking echocardiography: concensus document of the EACVI/ASE/Industry Task Force to standardize deformation imaging. Eur heart J-Cardiovasc Imag 16 (2015): 1-11.
30. Cossio-Aranda J, Zamora K, Nanda NC, Uzendu A, Keirns C, Verdejo-Paris J, Martinez-Rios MA, Espinola-Zavaleta N. Echocardiographic correlates of severe pulmonary hypertension in adult patients with ostium secundum atrial septal defect. Echocardiography 33 (2016): 1891-1896.
31. Utsunomiya H, Nakatani S, Okada T, Kanzaki H, Kyotani S, Yamamoto H, Nakanishi N, Kihara Y, Kitakaze M. Abstract 2436: Tricuspid E/Ea is a Powerful Predictor of Cardiac Events in Patients with Chronic Pulmonary Hypertension. Circulation 118 (2008): S_726-S_726.
32. Stephensen S, Steding-Ehrenborg K, Munkhammar P, Heiberg E, Arheden H, Carlsson M. The relationship between longitudinal, lateral, and septal contribution to stroke volume in patients with pulmonary regurgitation and healthy volunteers. Am J Physiol Heart Circ Physiol 306 (2014): H895-903.
33. Li Y, Wang Y, Meng X, Zhu W, Lu X. Assessment of right ventricular longitudinal strain by 2D speckle tracking imaging compared with RV function and hemodynamics in pulmonary hypertension. Int J Cardiovasc Imaging 33 (2017): 1737-1748.
34. Puwanant S, Park M, Popovic ZB, Tang WH, Farha S, George D, Sharp J, Puntawangkoon J, Loyd JE, Erzurum SC, Thomas JD. Ventricular geometry, strain, and rotational mechanics in pulmonary hypertension. Circulation 121 (2010): 259-66.
35. Jategaonkar SR, Scholtz W, Butz T, Bogunovic N, Faber L, Horstkotte D. Two-dimensional strain and strain rate imaging of the right ventricle in adult patients before and after percutaneous closure of atrial septal defects. Eur J Echocardiogr 10 (2009): 499-502.
36. Pham T, Nisbet L, Taberner A, Loiselle D, Han JC. Pulmonary arterial hypertension reduces energy efficiency of right, but not left, rat ventricular trabeculae. J Physiol 596 (2018): 1153-1166.

37. Korstjens IJ, Rouws CH, van der Laarse WJ, Van der Zee L, Stienen GJ. Myocardial force development and structural changes associated with monocrotaline induced cardiac hypertrophy and heart failure. J Muscle Res Cell Motil 23 (2002): 93-102.
38. Kogler H, Hartmann O, Leineweber K, Nguyen van P, Schott P, Brodde OE, Hasenfuss G. Mechanical load-dependent regulation of gene expression in monocrotaline-induced right ventricular hypertrophy in the rat. Circulation Res 93 (2003): 230-7.
39. Hardziyenka M, Campian ME, Reesink HJ, Surie S, Bouma BJ, Groenink M, Klemens CA, Beekman L, Remme CA, Bresser P, Tan HL. Right ventricular failure following chronic pressure overload is associated with reduction in left ventricular mass: evidence for atrophic remodeling. J Am Coll Cardiol 57 (2011): 921-8.
40. Daicho T, Yagi T, Abe Y, Ohara M, Marunouchi T, Takeo S, Tanonaka K. Possible involvement of mitochondrial energy-producing ability in the development of right ventricular failure in monocrotaline-induced pulmonary hypertensive rats. J Pharmacol Sci 111 (2009): 33-43.
41. Handoko ML, de Man FS, Happe CM, Schalij I, Musters RJ, Westerhof N, Postmus PE, Paulus WJ, van der Laarse WJ, Vonk-Noordegraaf A. Opposite effects of training in rats with stable and progressive pulmonary hypertension. Circulation 120 (2009): 42-9.
42. Krayenbuehl HP, Turina J, Hess O. Left ventricular function in chronic pulmonary hypertension. Am J Cardiol 41 (1978): 1150-8.
43. Dempsie Y, MacLean MR. The influence of gender on the development of pulmonary arterial hypertension. Exp Physiol 98 (2013): 1257-61.
44. Lahm T, Tuder RM, Petrache I. Progress in solving the sex hormone paradox in pulmonary hypertension. Am J Physiol Lung Cell Mol Physiol 307 (2014): L7-26.
45. Mair KM, Johansen AK, Wright AF, Wallace E, MacLean MR. Pulmonary arterial hypertension: basis of sex differences in incidence and treatment response. Br J Pharmacol 171 (2014): 567-79.
46. Marra AM, Benjamin N, Eichstaedt C, Salzano A, Arcopinto M, Gargani L, D Alto M, Argiento P, Falsetti L, Di Giosia P, Isidori AM, Ferrara F, Bossone E9, Cittadini A, Grünig E. Gender-related differences in pulmonary arterial hypertension targeted drugs administration. Pharmacol Res 114 (2016): 103-109.